Journal of Metals, Materials and Minerals, 36(3), e2595, 2026

Enhanced red emission of $Gd_2MoO_6:Eu^{3+}$ phosphor-in-glass embedded in SiO_2-TeO_2-Na_2O-BaO matrix for solid-state lighting

Patarawagee YASAKA[1,2,*], Winut WONGWAN[1,2], Seubsakun KHONDARA[1,2], and Jakrapong KAEWKHAO[1,2]

[1] *Center of Excellence in Glass Technology and Materials Science (CEGM), Nakhon Pathom Rajabhat University, Nakhon Pathom, 73000, Thailand*
[2] *Physics Program, Faculty of Science and Technology, Nakhon Pathom Rajabhat University, 73000, Thailand*

***Corresponding author e-mail**: pyasaka@webmail.npru.ac.th

Received date:
4 December 2025
Revised date:
15 December 2025
Accepted date:
22 March 2026

Keywords:
Phosphor-in-glass;
Photoluminescence;
Europium

Abstract

$Gd_2MoO_6:Eu^{3+}$ phosphor-in-glass (PIG) composites were synthesized by a microwave-assisted melting technique using a $50SiO_2$:$20TeO_2$:$15Na_2O$:15BaO glass matrix containing 0.00 wt% to 10.00 wt% phosphor. Their structural, optical, and luminescent properties were systematically investigated. X-ray diffraction confirmed the formation of crystalline Gd_2MoO_6 phases, which became prominent at 5.00 wt% and 10.00 wt%, indicating partial crystallization within the glass network. The density and refractive index increased from 3.621 g·cm^{-3} to 3.774 g·cm^{-3} and 1.535 to 1.692 with higher phosphor loading, suggesting a more compact structure. Absorption spectra showed four characteristic Eu^{3+} bands at 464 nm, 534 nm, 2088 nm, and 2203 nm, while excitation monitored at 613 nm exhibited the strongest band at 394 nm ($^7F_0 \rightarrow {}^5L_6$). Emission spectra revealed intense red emissions at 590 nm, 613 nm, 653 nm, and 702 nm, corresponding to the $^5D_0 \rightarrow {}^7F_1$–$^7F_5$ transitions, with chromaticity coordinates of (x, y) = (0.65, 0.34). The photoluminescence lifetime, measured under 394 nm excitation and monitored at 613 nm emission, decreased slightly from 1.719 ms to 1.585 ms. Vickers hardness values measured under a 0.2 kgf load ranged from 1601.7 HV0.2 to 1606.1 HV0.2, indicating high mechanical durability. Overall, the obtained PIG composites show strong red emission and robust structural properties, demonstrating their potential for solid-state lighting applications.

1. Introduction

In recent years, solid-state lighting (SSL) such as light-emitting diodes (LEDs) has become very popular as a replacement for traditional lamps. LEDs are small, bright, energy-saving, and have a long lifetime [1]. However, long-term use can cause problems because the resin used to cover the phosphor layer can degrade by heat, leading to lower brightness and color change. To solve this, inorganic materials such as transparent ceramics, single crystals, and phosphor-in-glass (PIG) are used instead of resin [2]. Among these materials, PIG is very attractive because it is easy to make, low-cost, and has high thermal and chemical stability [3,4].

Phosphor-in-glass combines the advantages of both phosphor and glass. The phosphor provides light emission, while the glass gives strong mechanical strength and protects the phosphor from heat and moisture. The type of glass used as the host is a key factor that affects light performance. Tellurite-based glass is especially interesting because it has low melting point, low phonon energy and a high refractive index, which helps to reduce non-radiative loss and improve light emission efficiency [5,6]. When modifying the composition, each oxide contributes specific benefits to the glass network. SiO_2 strengthens the glass network, provides good transparency, and improves chemical durability. Na_2O, acting as a network modifier, adjusts thermal and mechanical properties, while BaO increases density, refractive index, and structural integrity [7]. These combined effects make the SiO_2–TeO_2–Na_2O–BaO system an excellent host matrix for luminescent applications.

Rare-earth elements, especially europium (Eu^{3+}), are widely used in red-emitting phosphors. The Eu^{3+} ion emits bright red light at around 615 nm due to its 5D0 → 7F2 electronic transition [8,9]. This sharp red emission is suitable for display and lighting applications. Molybdate-based compounds such as Gd_2MoO_6 have attracted considerable interest due to their excellent optical and luminescent properties. These materials have been widely studied as phosphor hosts, scintillators, and optical materials because of their high chemical stability and efficient energy transfer capability. In addition, Gd^{3+} ions can act as sensitizers that facilitate energy transfer to activator ions, which enhances luminescence efficiency [10–13].

In this work, $Gd_2MoO_6:Eu^{3+}$ phosphor was embedded into SiO_2:TeO_2:Na_2O:BaO glass matrix to form a phosphor-in-glass composite. The samples were prepared using the microwave-assisted melting method, which offers fast, uniform heating and shorter synthesis time compared to conventional melting [14–16]. This method helps to mix the phosphor evenly inside the glass and maintain high transparency. The structural, optical, and luminescent properties of the prepared samples were studied to find the best composition for strong red emission. The results can be useful for developing high-efficiency solid-state lighting and related optical devices.

2. Experimental

2.1 Sample preparation

$Gd_{1.9}MoO_6$:0.1Eu_2O_3 phosphors in a 50SiO_2:20TeO_2:15Na_2O: 15BaO glass with varying phosphor contents (0.00 wt%, 1.00 wt%, 2.00 wt%, 5.00 wt%, and 10.00 wt%) were synthesized using a microwave sintering technique. The preparation process consisted of three main steps.

First, the phosphor preparation was performed by weighing high-purity Gd_2O_3, MoO_3, and Eu_2O_3 powders according to the stoichiometric ratio. The raw materials were mixed using a wet ball mill at 300 rpm for 6 h to achieve homogeneous blending. The obtained mixture was then calcined at 500°C for 12 h to remove residual moisture, promote the solid-state reaction, and initiate phase formation of Gd_2MoO_6. After calcination, the material was ground into fine powder to increase surface area and ensure uniform sintering. The powder was then sintered at 900°C for 12 h to achieve complete crystallization. The crystal structure of the synthesized phosphor was examined by X-ray diffraction (XRD) to confirm the formation of the Gd_2MoO_6:Eu^{3+} phase.

Next, the glass preparation was prepared using the composition 50SiO_2:20TeO_2:15Na_2O:15BaO (mol%). The raw materials were weighed and mixed in an alumina crucible and melted at 1200°C. The molten glass was poured into a graphite mold and annealed at 500°C for 3 h to remove internal stress. The samples were then slowly cooled to room temperature.

Finally, the phosphor-in-glass composite was prepared by mixing the synthesized phosphor powder with the prepared glass and melting the mixture using a microwave at 1000 W for 20 min. The molten mixture was poured into a graphite mold, annealed again at 500°C for 3 h, and allowed to cool to room temperature, as shown in Figure 1. The prepared samples were cut and polished into 1 cm × 1.5 cm × 0.3 cm specimens for structural, optical, and luminescence characterization, as shown in Figure 2. When the amount of phosphor increased the samples became less transparent. The sample with 10.00 wt% phosphor looked cloudy because too much phosphor affected the glass structure. When the phosphor content was higher than 10.00 wt% the glass and phosphor phases could not form a uniform or well-bonded structure. The opacity observed at high phosphor loading can be attributed to crystallization within the glass matrix. Similar behavior has been reported in phosphor-in-glass systems, where excessive phosphor incorporation induces crystallization of glass constituents, leading to increased light scattering and loss of transparency [11].

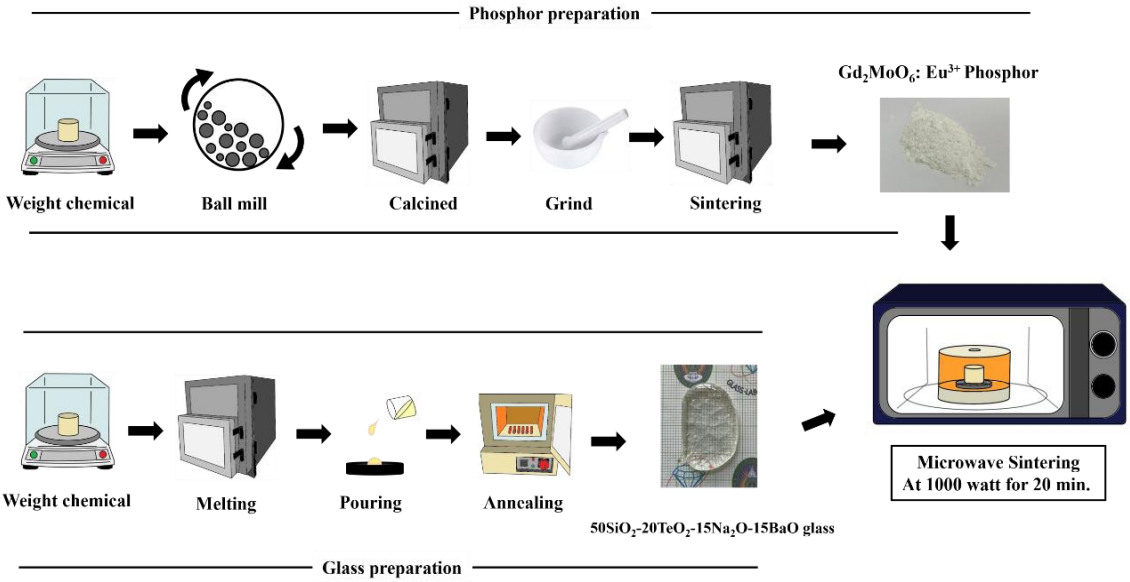

Figure 1. Preparation process of Gd_2MoO_6:Eu^{3+} phosphors in SiO_2:TeO_2:Na_2O: BaO glass by microwave sintering.

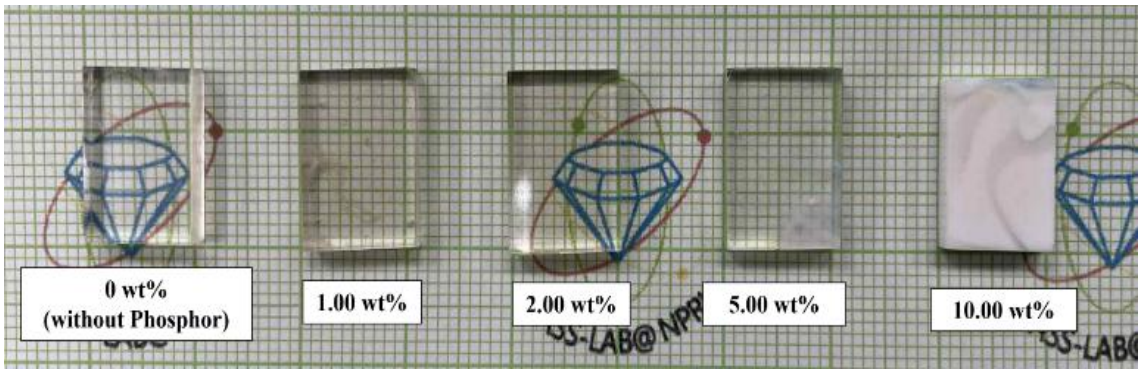

Figure 2. The Gd_2MoO_6:Eu^{3+} phosphors-in SiO_2: TeO_2:Na_2O:BaO glass with different weights of phosphor.

2.2 Characterization

The prepared phosphor-in-glass (PIG) samples were examined using several analytical instruments to evaluate their physical, structural, optical, and luminescent properties. The density (ρ) of each sample was measured with a precision density kit attached to a four-digit microbalance.

The refractive index (n) was determined using a Presidium Refractive Index Meter II.

For structural characterization, X-ray diffraction (XRD) patterns were obtained on a Shimadzu XRD-6100 diffractometer operating at 40 kV and 30 mA to analyze both glassy and powdered specimens. The microhardness of the PIG samples was evaluated using an HVS-1000 Digital Micro Vickers Hardness Tester to assess their mechanical durability.

The optical absorption, transmittance (%T) were recorded in the 200 nm to 3300 nm wavelength range using a Shimadzu UV-3600 UV-Vis-NIR spectrophotometer. The photoluminescence (PL) emission and decay lifetime measurements were carried out on a Cary Eclipse fluorescence spectrophotometer within the 200 nm to 900 nm spectral range to investigate the luminescence behavior of the samples.

3. Results and discussion

3.1 X-ray diffraction (XRD)

The X-ray diffraction (XRD) analysis of the phosphor-in-glass samples with different phosphor contents was performed. The results showed that when the amount of phosphor increased, crystal peaks were found around 30° and 50°. These peaks were especially visible in the samples containing 5.00 wt% and 10.00 wt%, as shown in Figure 3. When compared with the reference pattern of Gd_2MoO_6 (PDF#00-024-0423), the diffraction peaks matched as shown in Figure 4. This result confirms that the phosphor was successfully incorporated into the glass matrix. However, at 10.00 wt% the sample became opaque, which may be due to the higher amount of phosphor causing more crystallization in the glass.

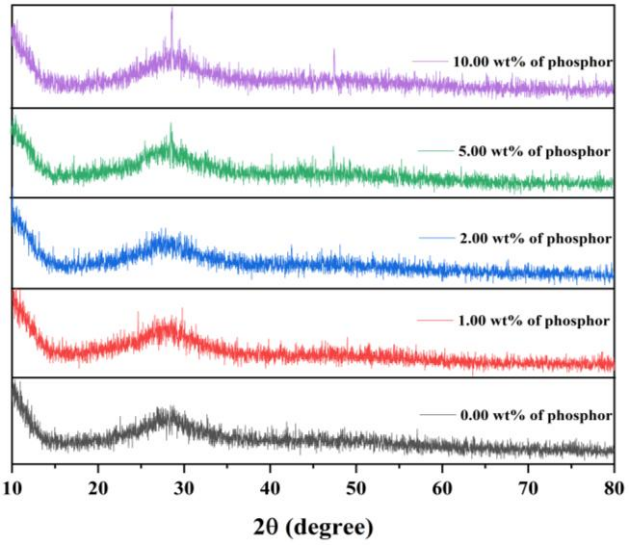

Figure 3. The X-ray diffraction of $Gd_2MoO_6:Eu^{3+}$ phosphors-in SiO_2:TeO_2:Na_2O:BaO glass.

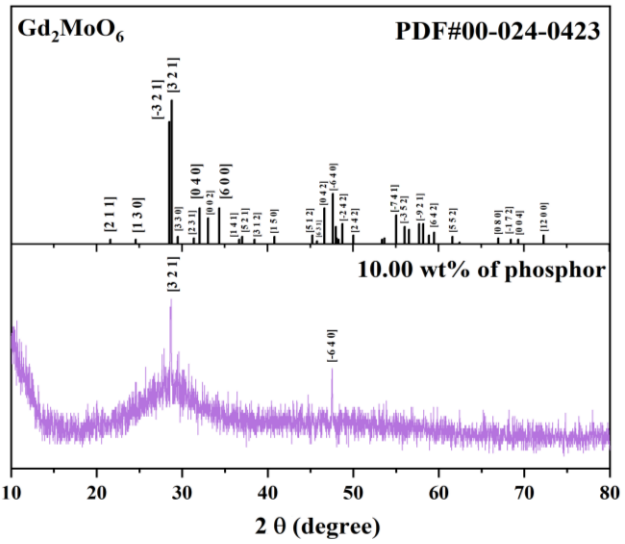

Figure 4. The $Gd_2MoO_6:Eu^{3+}$ phosphors-in SiO_2:TeO_2:Na_2O:BaO glass compare with Gd_2MoO_6 standard reference.

3.2 Density, molar volumes, refractive index, and vickers hardness

The density of the phosphor-in-glass (PIG) samples was measured according to the Archimedes' principle. In this method, each glass specimen was weighed in air and then in distilled water to determine its buoyant loss. The density (ρ) was obtained from the equation:

$$\rho_{\text{samples}} = \frac{W_{\text{Air}}}{W_{\text{Air}} - W_{\text{Liquid}}} \times \rho_{\text{Liquid}} \quad (1)$$

Where W_{Air} and W_{Liquid} represent the sample weights in air and in water, respectively, and ρ_{Liquid} is the density of distilled water at room temperature (1 g·cm^{-3}). The measured density values for the samples containing 0 wt%, 1 wt%, 2 wt%, 5 wt%, and 10 wt% phosphor were 3.621 g·cm^{-3}, 3.646 g·cm^{-3}, 3.649 g·cm^{-3}, 3.656 g·cm^{-3}, and 3.774 g·cm^{-3}, respectively. Figure 5 shows the variation of density, molar volume, and refractive index of the samples as a function of phosphor concentration. The density slightly increases from approximately 3.62 g·cm^{-3} to 3.77 g·cm^{-3} as the phosphor content increases. This increase can be attributed to the incorporation of Gd_2MoO_6 phosphor, which contains relatively heavy elements such as Gd and Mo, resulting in a higher overall mass of the glass system. At the same time, the molar volume gradually increases with increasing phosphor content. Since the molar volume is defined as $V_m = M/\rho$, the addition of Gd_2MoO_6 with a higher molar mass compared with the glass components leads to an increase in the total molecular weight of the system, which contributes to the observed increase in molar volume. The increase in molar volume suggests that the incorporation of phosphor modifies the packing arrangement of the structural units in the glass network. The refractive index also increases with increasing phosphor concentration, rising from 1.535 to 1.692 for samples containing 0.00 wt% to 5.00 wt% phosphor. According to the relation $n = c/v$, where c is the speed of light in vacuum and v is the speed of light in the material, a higher optical density reduces the velocity of light in the medium and results in a higher refractive index. A similar trend has been reported in rare-earth-doped glasses, where the density, molar volume, and refractive index

increase with increasing dopant concentration due to the incorporation of heavier ions and modification of the glass network structure [17].

The Vickers hardness values of the phosphor-in-glass samples were measured under a loading condition of HV0.2. The obtained hardness values are approximately 3.14 GPa to 3.15 GPa for phosphor contents ranging from 0.00 wt% to 10.00 wt%, as summarized in Table 1. The results show that the hardness values remain almost unchanged with increasing phosphor content, indicating that the incorporation of phosphor has little effect on the mechanical hardness of the glass matrix.

For comparison, Table 1 also includes previously reported phosphor-in-glass systems. The Sr_2ZnMoO_6:Sm_2O_3 phosphor-in TeO_2-ZnO-B_2O_3 glass reported in our previous work exhibits a hardness value of about 3.03 GPa [14], which is comparable to the values obtained in the present study. This comparison indicates that the newly developed glass host maintains similar mechanical strength while employing a different glass composition. Furthermore, Eu^{3+}-doped TeO_2-based glasses reported in the literature show hardness values in the range of 2.77 GPa to 3.19 GPa [18–20], which are also comparable to those of the present samples. In contrast, the ZBS-2Eu glass system based on a SiO_2 host exhibits a higher hardness value of about 4.09 GPa [21]. This difference suggests that the vickers hardness is mainly governed by the glass host composition. Overall, these results indicate that the mechanical hardness of phosphor-in-glass materials is largely determined by the glass matrix, while the incorporation of phosphor has only a minor influence on the hardness of the samples.

3.3 Absorption studies

The absorption properties of the prepared glass samples were investigated at room temperature in the wavelength range of 350 nm to 2300 nm. As shown in Figure 6, several absorption bands were observed at 464 nm, 534 nm, 2088 nm, and 2203 nm. These absorption bands are attributed to the characteristic electronic transitions of Eu^{3+} ions, corresponding to the transitions from the ground state to the excited states of 5D2, 7F1, and 7F6, as well as the 7F1 → 7F6 transition, espectively. After the incorporation of phosphor into the glass matrix, additional absorption peaks appeared at several wavelengths, particularly in the region of 625 nm to 1000 nm. These peaks correspond to the characteristic absorption transitions of Eu^{3+} ions originating in the phosphor. This result indicates that Eu^{3+} ions from the phosphor are successfully introduced into the glass matrix and contribute to the optical absorption behavior of the samples. Moreover, the intensity of the absorption bands increases with increasing phosphor content.

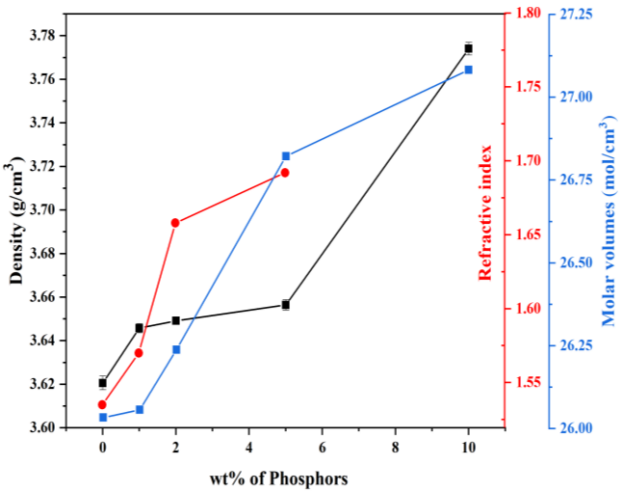

Figure 5. The Density, Molar volumes, and Refractive index of Gd_2MoO_6:Eu^{3+} phosphors-in SiO_2:TeO_2:Na_2O:BaO glass with different weights of phosphor.

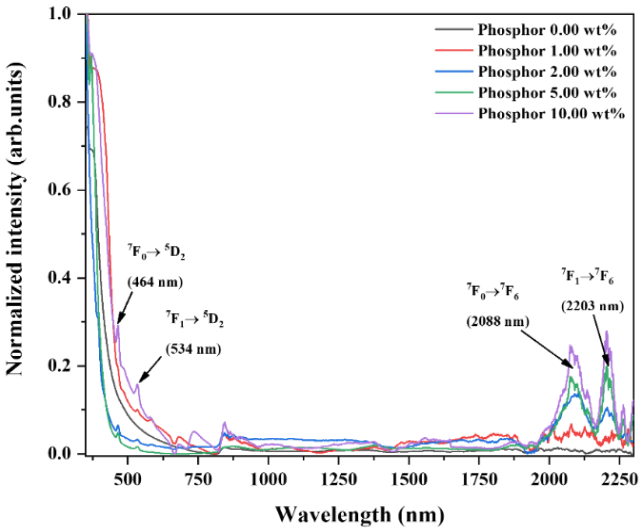

Figure 6. Absorption spectra of Gd_2MoO_6:Eu^{3+} phosphors-in SiO_2:TeO_2:Na_2O:BaO glass.

Table 1 Vickers Hardness (HV0.2) Comparison of Phosphor-in-Glass Materials.

Samples	Vickers hardness [Gpa]	References
Phosphor 0.00 wt%	3.14	Present work
Phosphor 1.00 wt%	3.14	Present work
Phosphor 2.00 wt%	3.15	Present work
Phosphor 5.00 wt%	3.15	Present work
Phosphor 10.00 wt%	3.15	Present work
Sr_2ZnMoO_6:Sm_2O_3 phosphor-in TeO_2:ZnO:B_2O_3 glass	3.03	[14]
Gd_2MoO_6:Eu^{3+} phosphor-in TeO_2:ZnO:BaO glass	3.07	[11]
Eu^{3+} doped TeO_2:Na_2O:MgO	2.77–2.93	[18]
ZBaT glass	2.89–3.19	[19]
TeO_2:15ZnO:15Na_2O	2.6	[20]
ZBS-2Eu	4.09	[21]

This trend suggests that a higher concentration of Eu^{3+} ions is present in the glass matrix, resulting in stronger optical absorption. The increase in absorption can also be explained by the shielding effect of the outer electron shells, which affects how the 4f electrons of the rare-earth ions interact with their surroundings [22]. The shielding effect refers to the protection of the inner 4f electrons of rare-earth ions by the outer 5s2 and 5p6 electron shells. Because of this shielding, the 4f electrons interact only weakly with the surrounding glass network or. crystal field. As a result, the 4f-4f transitions appear as relatively sharp absorption bands and are less sensitive to the local structural environment [23]

3.4 Photoluminescence studies

The excitation spectra were used to study the energy levels of Eu^{3+} ion and to find the best wavelength for measuring the luminescence of the prepared samples. As shown in Figure 7, the excitation spectra recorded at an emission wavelength of 613 nm shows seven peaks at 362 nm, 382 nm, 394 nm, 414 nm, 465 nm, 526 nm, and 533 nm. These peaks correspond to the transitions of Eu^{3+} ion from the ground state $^7F_0$ to the excited states 5D4, 5L7, 5L6, 5D3, 5D2, 5D1, and 7F1→5D1, respectively [24]. Among them, the band at 465 nm had the highest intensity, so it was chosen as the excitation wavelength for the emission study. The emission spectra under 465 nm excitation are shown in Figure 8. Four emission peaks were found at 590 nm, 613 nm, 653 nm, and 702 nm, which correspond to the transitions 5D0→7F1, 5D0→7F2, 5D0→7F3, and 5D0→7F5 of Eu^{3+} ion as shown in Figure 9. The emission intensity increased when more phosphor was added, meaning that more Eu^{3+} ion took part in the light emission process. However, due to the mixing limit between phosphor and glass, it was not possible to add more than 10.00 wt% phosphor. Although the sample containing 10.00 wt% phosphor becomes opaque, the photoluminescence observed in this study mainly originates from the phosphor incorporated into the glass matrix. Therefore, the transparency of the glass does not directly affect the intrinsic emission of the phosphor. The color of the light emission for the 10.00 wt% sample was analyzed using the CIE 1931 color diagram, as shown in Figure 10. The chromaticity coordinates were (x, y) = (0.65, 0.34), representing a reddish color. This confirms that the light emitted from the samples mainly comes from the red emission of Eu^{3+} ion. The photoluminescence lifetime of Gd_2MoO_6: Eu^{3+} phosphors in the glass matrix, measured under 394 nm excitation and monitored at 613 nm emission, is shown in Figure 11. The lifetimes were 1.719 ms, 1.693 ms, 1.601 ms, and 1.585 ms for 1.00 wt%, 2.00 wt%, 5.00 wt%, and 10.00 wt% phosphor, respectively. The decrease in lifetime with increasing phosphor content can be explained by cross-relaxation energy transfer between adjacent Eu^{3+} ion. In this process, an excited Eu^{3+} ion transfers part of its energy to a neighboring ion in the ground state, leading to non-radiative decay. As the concentration of Eu^{3+} increases, the distance between ions becomes smaller, making cross-relaxation more likely [7,25]. These results show that all samples maintain strong red emission and stable decay behavior across the studied compositions, confirming that the phosphor-in-glass system is a promising red-emitting material for solid-state lighting applications.

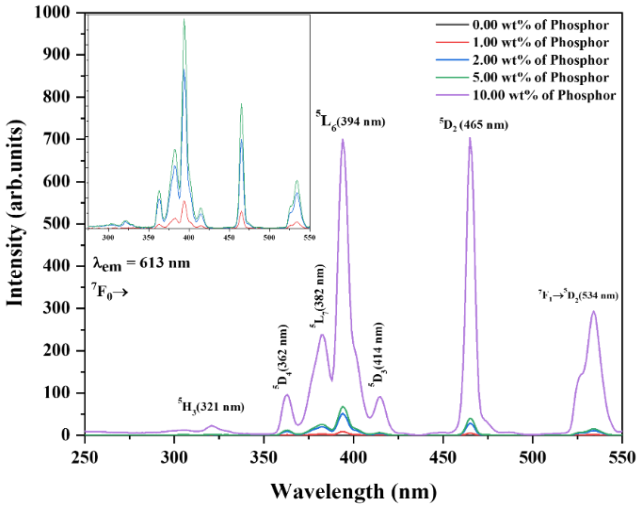

Figure 7. The excitation spectra of $Gd_2MoO_6:Eu^{3+}$ phosphors-in SiO_2:TeO_2:Na_2O:BaO glass.

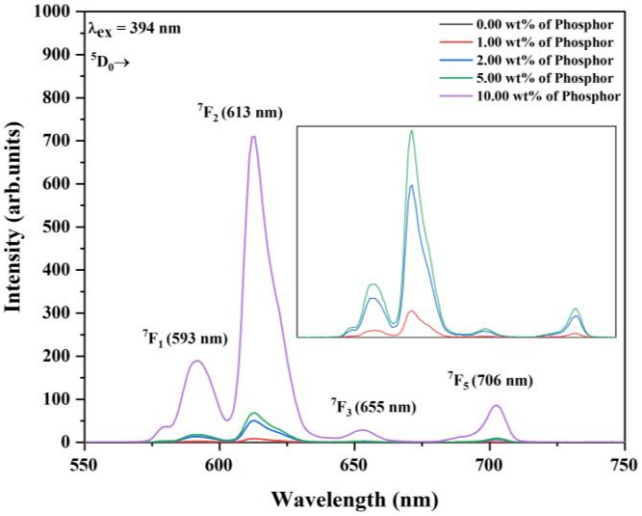

Figure 8. The emission spectra of $Gd_2MoO_6:Eu^{3+}$ phosphors-in SiO_2:TeO_2:Na_2O:BaO glass.

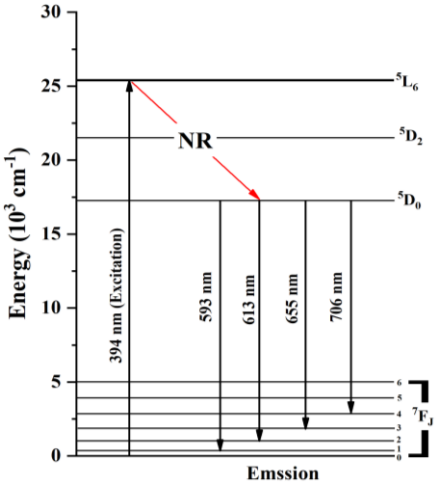

Figure 9. Energy level diagram of Eu^{3+} ion under excited at 394 nm.

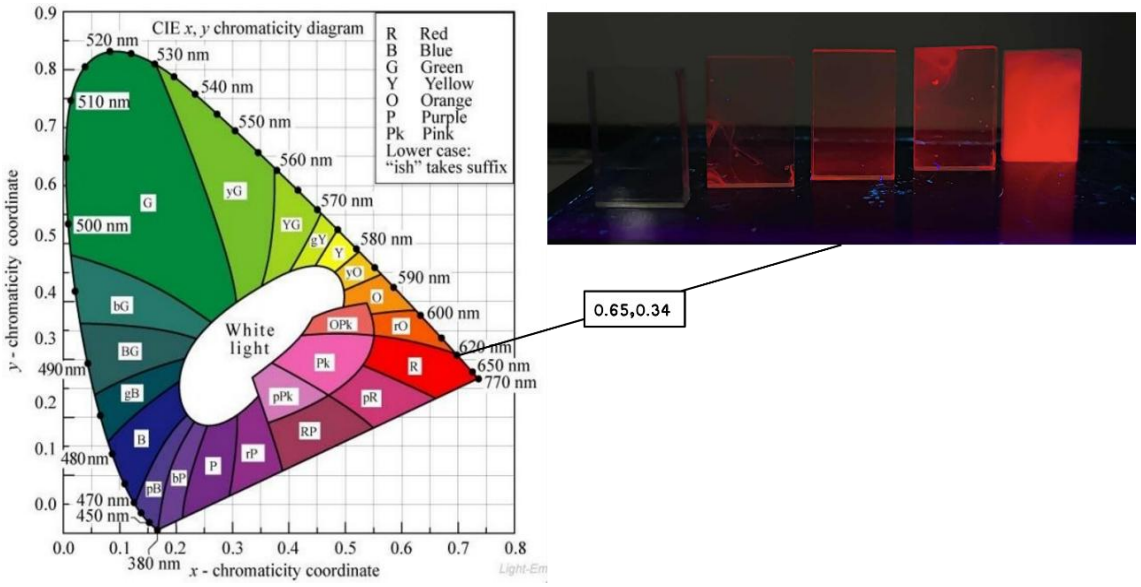

Figure 10. CIE 1931 of $Gd_2MoO_6:Eu^{3+}$ phosphors-in $SiO_2:TeO_2:Na_2O:BaO$ glasses.

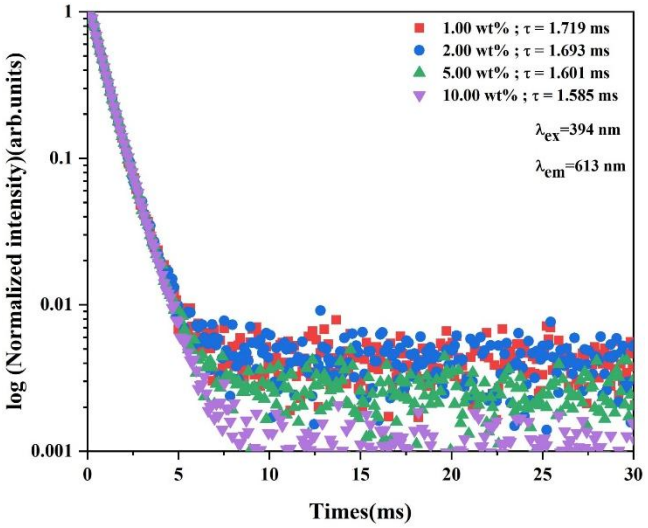

Figure 11. The lifetime of $Gd_2MoO_6:Eu^{3+}$ phosphors-in $SiO_2:TeO_2:Na_2O:BaO$ glass.

4. Conclusion

$Gd_2MoO_6:Eu^{3+}$ phosphor-in-glass composites were successfully prepared by a microwave-assisted melting method using a $50SiO_2$:$20TeO_2$:$15Na_2O$:15BaO glass matrix. XRD patterns confirmed the formation of crystalline Gd_2MoO_6 phases, with peak intensities increasing significantly at 5.00 wt% and 10.00 wt% phosphor contents. The density and refractive index increased slightly with phosphor loading, indicating structural modification of the glass network. The optical spectra showed four characteristic absorption bands of Eu^{3+} at 464 nm, 534 nm, 2088 nm, and 2203 nm, while excitation at 465 nm yielded strong red emission with four main peaks at 590 nm, 613 nm, 653 nm, and 702 nm.

Glass samples containing 0 wt% to 5 wt% phosphor remained transparent with uniform phosphor dispersion, whereas the 10.00 wt% sample became opaque but exhibited the strongest emission intensity with chromaticity coordinates (x, y) = (0.65, 0.34). The average luminescence lifetimes decreased from 1.719 ms to 1.585 ms with increasing phosphor concentration. The Vickers hardness values measured under a 0.2 kgf load (HV0.2) ranged from 1601.7 HV0.2 to 1606.1 HV0.2, indicating high mechanical durability and improved hardness compared with previously reported phosphor-in-glass systems.

These results demonstrate that microwave-assisted melting provides a fast and effective route for synthesizing phosphor-in-glass composites that combine strong red luminescence, good transparency at moderate phosphor levels, and high mechanical robustness, highlighting their potential for solid-state lighting applications.

Acknowledgements

The authors acknowledge Nakhon Pathom Rajabhat University and Thailand Science Research and Innovation (TSRI) for providing the necessary facilities and resources that enabled the successful completion of this study.

References

[1] X. Pang, H. Zhang, L. Xie, T. Xuan, Y. Sun, S. Shuaichen, B. Jiang, W. Chen, J. Zhuang, C. Hu, Y. L. Liu, B. Lei, and X. Zhang, "Precipitating $CsPbBr_3$ quantum dots in boro-germanate glass with a dense structure and inert environment toward highly stable and efficient narrow-band green emitters for wide-color-gamut liquid crystal displays," *Journal of Materials Chemistry C*, vol. 7, no. 42, pp. 13139–13148, 2019.

[2] S. Selvi, K. Marimuthu, and G. Muralidharan, "Effect of PbO on the B_2O_3–TeO_2–P_2O_5–BaO–CdO–Sm_2O_3 glasses - Structural and optical investigations," *Journal of Non-Crystalline Solids*, vol. 461, pp. 35–46, 2017.

[3] P. Zheng, S. Li, L. Wang, T-L. Zhou, S. You, T. Takeda, N. Hirosaki, and R-J. Xie, "Unique color converter architecture enabling phosphor-in-glass (PiG) films suitable for high-power and high-luminance laser-driven white lighting," *ACS Applied Materials & Interfaces*, vol. 10, no. 17, pp. 14930–14940, 2018,

[4] Y. Peng, R. Li, S. Wang, Z. Chen, L. Nie, and M. Chen, "Luminous Properties and thermal reliability of screen-printed phosphor-in-glass-based white light-emitting diodes," *IEEE Transactions on Electron Devices*, vol. 64, no. 3, pp. 1114–1119, 2017.

[5] P. Yasaka, R. Rajaramakrishna, W. Wongwan, P. Yamchumporn, H. J. Kim, and J. Kaewkhao, "Development of ZnO–BaO–B_2O_3–TeO_2 glass doped with Sm^{3+} for orange emitting material," *Solid State Sciences*, vol. 98, 2019.

[6] W. Thanyaphirak, P. Yasaka, K. Boonin, N. Sangwaranatee, and J. Kaewkhao, "Dy^{3+} ion - doped zinc barium niobium boro-tellurite glasses: Structural, optical, and luminescence insights for white light applications," *Suranaree Journal of Science and Technology*, vol. 31, no. 3, pp. 1–9, 2024.

[7] W. Wongwan, P. Yasaka, K. Boonin, A. Angnanon, N. Intachai, and S. Kothan, "Optimization of energy transfer in Tb^{3+}/Sm^{3+} ions doped silicoborotellurite scintillation glass for X-ray imaging application," *Radiation Physics and Chemistry*, vol. 237, no. June, p. 113124, 2025.

[8] P. Krongkitsiri, P. Yasaka, K. Boonin, W. Wongwan, and J. Kaewkhao, "Synthesis and luminescence properties of Sr_2ZnMoO_6:Eu_2O_3 phosphors," *Journal of Physics: Conference Series,* vol. 2602, no. 1, pp. 2–8, 2023.

[9] I. I. Kindrat, and B. V. Padlyak, "Luminescence properties and quantum efficiency of the Eu-doped borate glasses," *Optical Materials (Amst).*, vol. 77, pp. 93–103, 2018.

[10] F. Lei, B. Yan, H. H. Chen, and J. T. Zhao, "Molten salt synthesis, characterization, and luminescence properties of $Gd_2MO_6:Eu^{3+}$ (M=W, Mo) phosphors," *Journal of the American Ceramic Society,* vol. 92, no. 6, pp. 1262–1267, 2009.

[11] P. Yasaka, W. Wongwan, K. Boonin, N. Intachai, S. Kothan, and A. Angnanon, "Microwave synthesis of Eu^{3+} ion doped phosphor in glass : A novel scintillation material with luminescence enhancement," *Radiation Physics and Chemistry*, vol. 237, no. June, p. 113106, 2025.

[12] G. Li, Z. Wang, Z. Quan, X. Liu, M. Yu, R. Wang, and J. Lin, "Sol-gel growth of $Gd_2MoO_6:Eu^{3+}$ nanocrystalline layers on SiO_2 spheres (SiO_2@$Gd_2MoO_6:Eu^{3+}$) and their luminescent properties," *Surface Science*, vol. 600, no. 16, pp. 3321–3326, 2006,

[13] M. Pang, X. Liu, and J. Lin, "Luminescence properties of $R_2MoO_6:Eu^{3+}$ (R = Gd, Y, La) phosphors prepared by Pechini sol-gel process," *Journal of Materials Research*, vol. 20, no. 10, pp. 2676–2681, 2005.

[14] W. Wongwan, P. Yasaka, K. Boonin, H. J. Kim, N. Discharoen, S. Kothan, and J. Kaewkhao, "Microwave-assisted fabrication of Sr_2ZnMoO_6:Sm_2O_3 phosphors in TeO_2:ZnO:B_2O_3 glass matrix for high-efficiency solid-state lighting applications," *Optik (Stuttg).*, vol. 297, p. 171532, 2023.

[15] W. Wongwan, P. Yasaka, K. Boonin, S. Khondara, H. J. Kim, S. Kothan, N. Chanlek, P. Kanjanaboos, N. Phuphathanaphong, T. Sareein, N. Sangwaranatee, and J. Kaewkhao, "A comparative study of microwave assisted and conventional melting techniques to glass properties," *Radiation Physics and Chemistry*, vol. 224, p. 112011, 2024,

[16] J. M. de Carvalho, C. C. S. Pedroso, M. S. de N. Saula, M. C. F. C. Felinto, and H. F. de Brito, "Microwave-assisted preparation of luminescent inorganic materials: A fast route to light conversion and storage phosphors," *Molecules*, vol. 26, no. 10, 2021.

[17] N. Jarucha, and P. Meejitpaisan, "Tb^{3+} concentration effect on the photo - and radioluminescence result of lanthanum borate glass for yellowish green laser application," *Suranaree J. Sci. Technol.*, vol. 30, no. 6, pp. 1–7, 2024.

[18] E. S. Sazali, M. R. Sahar, and S. K. Ghoshal, "Influence of europium ion on structural, mechanical and luminescence behavior of tellurite nanoglass," *Journal of Physics: Conference Series*, vol. 431, no. 1, 2013.

[19] P. Yasaka, Y. Ruangthaweep, P. Mangthong, and J. Kaewkhao, "Physical and optical investigation of ZnO-BaO-TeO_2 glass systems," *Materials Today: Proceedings*, vol. 5, no. 6, pp. 14199–14203, 2018.

[20] T. Watanabe, Y. Benino, and T. Komatsu, "Change in vickers hardness at the glass transition region for fragile and strong glasses," vol. 286, pp. 141–145, 2001.

[21] W. M. Cheong, M. H. M. Zaid, K. A. Matori, Y. W. Fen, T. S. Tee, Z. W. Loh, M. Z. H. Mayzan, and S. Schmid, "Influence of Eu^{3+} Ions on elastic moduli and microhardness of zinc - boro - soda - lime - silica glass system," *Silicon*, vol. 16, pp. 3173–3180, 2024.

[22] P. R. Rani, M. Venkateswarlu, K. Swapna, S. Mahamuda, M. V. V. K. S. Prasad, and A. S. Rao, "Spectroscopic and luminescence properties of Ho^{3+} ions doped barium lead alumino fluoro borate glasses for green laser applications," *Solid State Sciences*, vol. 102, p. 106175, 2020.

[23] E. M. A. Hussein, "Characterization of some radiation shielding, optical, and physical properties of fluorophosphate glasses modified by Sm^{3+}," *Journal of Materials Science: Materials in Electronics.*, vol. 32, no. 21, pp. 25933–25951, 2021.

[24] W. T. Carnall, P. R. Fields, and K. Rajnak, "Electronic energy levels of the trivalent lanthanide aquo ions. IV. Eu^{8+}," *Journal of Chemical Physics.*, vol. 49, no. 10, pp. 4424–4442, 1968.

[25] K. A. Kumar, S. Babu, V. R. Prasad, S. Damodaraiah, and Y. C. Ratnakaram, "Optical response and luminescence characteristics of Sm^{3+} and Tb^{3+}/sm^{3+} co-doped potassium-fluoro-phosphate glasses for reddish-orange lighting applications," *Materials Research Bulletin*, vol. 90, pp. 31–40, 2017.